Hindawi
Advances in Materials Science and Engineering
Volume 2017, Article ID 1750517, 10 pages
https://doi.org/10.1155/2017/1750517

Research Article

Influence of Impurities on the Radiation Response of the TlBr Semiconductor Crystal

Robinson Alves dos Santos,[1] Carlos Henrique de Mesquita,[1] Júlio Batista Rodrigues da Silva,[1] Caue de Melo Ferraz,[1] Fabio Eduardo da Costa,[1] João Francisco Trencher Martins,[1] Roseli Fernandes Gennari,[2] and Margarida Mizue Hamada[1]

[1]*Institute of Nuclear and Energy Research, IPEN-CNEN/SP, São Paulo, SP, Brazil*
[2]*Institute of Physics, IFUSP, São Paulo, SP, Brazil*

Correspondence should be addressed to Margarida Mizue Hamada; mmhamada@ipen.br

Received 1 June 2016; Revised 1 November 2016; Accepted 10 November 2016; Published 18 January 2017

Academic Editor: Pavel Lejcek

Two commercially available TlBr salts were used as the raw material for crystal growths to be used as radiation detectors. Previously, TlBr salts were purified once, twice, and three times by the repeated Bridgman method. The purification efficiency was evaluated by inductively coupled plasma mass spectroscopy (ICP-MS), after each purification process. A compartmental model was proposed to fit the impurity concentration as a function of the repetition number of the Bridgman growths, as well as determine the segregation coefficients of impurities in the crystals. The crystalline structure, the stoichiometry, and the surface morphology of the crystals were evaluated, systematically, for the crystals grown with different purification numbers. To evaluate the crystal as a radiation semiconductor detector, measurements of its resistivity and gamma-ray spectroscopy were carried out, using ^{241}Am and ^{13}3Ba sources. A significant improvement of the radiation response was observed in function of the crystal purity.

1. Introduction

The main physical semiconductor properties required for the production of room temperature semiconductor detectors are (a) high atomic number and density for high stopping power, (b) band gap large enough to maintain leakage currents low at room temperature, and (c) large mobility-lifetime products ($\mu\tau$) for electrons and holes aiming at efficient charge collection [1, 2]. TlBr has emerged as a particularly interesting material as room temperature semiconductor in view of its wide band gap (2.68 eV) and its large density (7.5 g/cm^3). TlBr crystals are composed of high atomic number elements (Z_{Tl} = 81 and Z_{Br} = 35) and show high resistivity (>10^{10} Ωcm) [2–8]. These are important factors in applications where compact and small thickness detectors are necessary for X- and gamma-ray measurements [2].

The performance of a radiation semiconductor detector depends on several factors related to the crystal quality, such as the carrier lifetime, mobility, crystallographic imperfections, and the impurity concentrations present in the crystal. Several studies on the preparation of TlBr detectors have been carried out and improvements in the methodology of purification, growth, and characterization of the crystals have been described, aiming to achieve all these factors [2–7]. However, as it can be observed in the literature [1, 8–12], the TlBr detector limitations are not yet completely resolved: primarily, the low collection efficiency of charge carriers, a fact that is probably caused by impurities and defects created in the crystal growth or in the surface treatment process. There is a consensus in the literature that the TlBr crystal purity is a crucial factor for its optimal performance as a radiation detector [2–6].

In this work, some aspects of the crystal impurity influence on the detector performance were evaluated by systematic measurements of the gamma-ray spectrometry

and resistivity. For purification, the crystal was grown by the Bridgman technique three times. The impurity decrease in the crystal was evaluated after each repetition number of the crystal growth, using the ICP-MS technique. The theory of compartments was used as a mathematical model to explain and to fit the data of the impurity concentration, as a function of the crystal growth repetition number.

2. Materials and Methods

Two commercially available TlBr salts (Merck and Sigma-Aldrich, in alphabetical order), with nominal purity of 99.99%, were used as the raw salt for crystal growths. In this work, the crystals were named Salt 1 and Salt 2, but, for the sake of business ethics, the results presented here do not identify their origin. TlBr crystals were grown by the vertical Bridgman technique, using quartz tubes as crucibles in vacuum atmosphere. Preliminarily, the quartz tubes were submitted to a chemical treatment. The tubes were previously washed with a cleaning agent solution (Extran MA 02, Merck) and, then, filled with a solution of hydrofluoric acid (5 per cent v/v); after 5 minutes, the tubes were rinsed three times with demineralized water. Subsequently, the quartz tubes were submitted to a thermal treatment at 650°C to avoid the adhesion of the crystals on the walls of the tubes. Afterward, the TlBr salt was introduced into one tube, evacuated to 10^{-6} Torr, and sealed off. The tube with TlBr was mounted into the vertical Bridgman furnace, where the TlBr was melted at a temperature of 550°C. Crystals of around 20 mm diameter and 60 mm length were obtained, with a growth rate of 1 mm/h. Following the same procedure, the crystals were grown repeatedly (three times) for purification. In this procedure, the impurities tend to migrate to the extremities of the crystal during the growth, due to the segregation of impurities along the crystal. Thus, better purity is expected to be found in the middle region. For each regrowth, the quartz tube was opened and two slice samples were taken from the crystals (Figure 1). The first sample migrated and it was taken for chemical analysis. The second sample was taken from the middle region of the ingot "middle," exactly 1.3 mm from the crystal middle, a region considered the prime region (~35 mm thick) of the crystal, assuming that good uniformity in the impurity concentrations exists in the middle region of the ingot. Samples (2 × 0.65 mm thick slices) were taken, adjacently, from the middle of the crystal, for chemical analysis and detector preparation. The "bottom" corresponds to the lower ingot extremity, which is cone-shaped (~20 mm thick).

A small amount of 50 mg was taken from the "top" region and the two 0.65 mm samplings of the "middle" region were used to identify and determine the concentration of impurities present in each region.

The impurity concentrations of the samples, taken from slices after each growth, were measured in an ICP-MS (inductively coupled plasma mass spectrometer, mod. Elan 6100 ICP-MS, PerkinElmer, USA). Previously, samples had been digested in a mixture of nitric acid (65%, Merck) and hydrogen peroxide (30%, Merck) by closed-vessel microwave digestion. Five impurity elements were found in the raw material: barium (Ba), calcium (Ca), lithium (Li), chromium (Cr), and copper (Cu). The concentrations of Cu and Cr in the raw material were already in their limit of detection (0.02 ppm for Cu and 0.04 ppm for Cr). The sample concentrations were determined through calibration with certified single reference material. The samples were measured in 10 replicates and the results represented by the arithmetic mean and the standard deviation (mean ± SD). The *Kruskal-Wallis One-Way Analysis of Variance on Ranks* was applied to identify significant differences among the crystal impurity concentrations, compared to those found in the raw salt. The statistical calculations were performed with the *SigmaStat for Windows Version 1.0* (Jandel Co. USA). The impurities were expressed in parts per million (ppm).

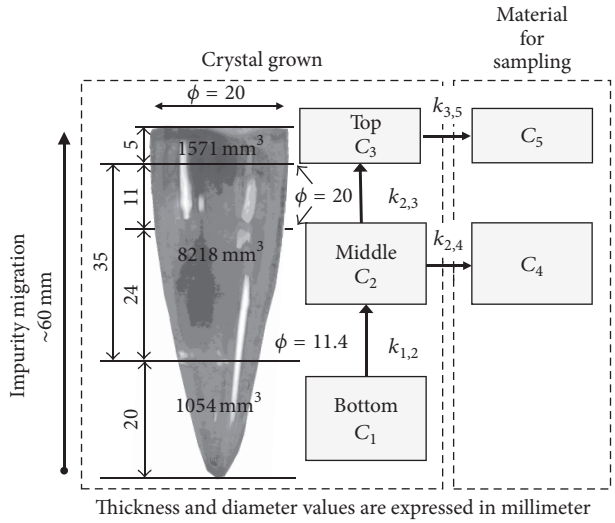

Figure 1: Compartmental model proposed to explain the migration of impurities in the TlBr crystal. The values of the constant $k_{i,j}$ are in Table 2.

The theory of compartments was used as a mathematical model to explain and to fit the data of the impurity concentration as a function of the crystal growth repetition number. In the mathematical basis of a generic compartmental model, the constants k will appear denoting the outputs ($k_{i,j}$) and inputs ($k_{j,i}$) for each compartment. In the present study, the C_2 compartment (the central region of the crystal) receives a fraction of the impurities from the lower region ($k_j = 1$, $i = 2$) and leaches its impurities ($k_i = 2$, $j = 3$) to the top compartment (C_3) or the upper region of the crystal. In the theory of compartmental analysis, it is assumed that the variation in the contents of the ith compartment C_i (here C_i = impurity concentration), as a function of the variable x (here x = number of growth repetitions), may be equated as follows:

$$\frac{dC_i(x)}{dx} = -\sum_{i=1;i\neq j}^{N} k_{i,j} \cdot C_i(x) + \sum_{j=1;j\neq i}^{N} k_{j,i} \cdot C_j(x), \quad (1)$$

where $k_{i,j}$ is the constant fraction of the impurity migration from the compartment (crystal region) i to compartment j, $k_{j,i}$ is the constant fraction of the impurity migration from the compartment j to compartment i, and N is the total number of compartments. Particularly, in this work, $N = 5$ and k constants are expressed as x^{-1}, that is, the inverse of Bridgman growth repetition number.

The compartmental model proposed in this work to explain the migration of impurities is shown in Figure 1. The C_1 compartment ($V_{C1} = 1054\,\text{mm}^3$) is assumed, physically, as being the bottom conical region which extends from zero to two millimeters in thickness ($\phi_{\text{minor}} = 2.2\,\text{mm}$, $\phi_{\text{major}} = 11.4\,\text{mm}$). The C_2 compartment ($V_{C2} = 8218\,\text{mm}^3$) is the middle region with 35 mm thickness, being 24 mm in the conical region ($\phi_{\text{minor}} = 11.4\,\text{mm}$, $\phi_{\text{major}} = 20\,\text{mm}$) and 11 mm in the cylindrical region ($\phi = 20\,\text{mm}$). The C_3 compartment ($1571\,\text{mm}^3$) corresponds to the top cylindrical region with 5 mm thickness ($\phi = 20\,\text{mm}$). The C_4 and C_5 compartments are located outside of the crystal region. They represent the material taken from the crystal for analysis. The accumulative C_4 compartment corresponds to the 1.3 mm thick slice samples, removed from C_2, at 1st, 2nd, and 3rd growth, used for chemical analysis and detector spectrometry characterization. The accumulative C_5 compartment refers to the 5 mm thick slice samples taken from C_3, at 1st, 2nd, and 3rd growth, to remove the top region where the impurities tend to migrate.

The core of this model, that is, the C_1, C_2, and C_3 compartments, may be defined, mathematically, as the first-order differential equation system, shown as follows:

$$\begin{aligned}\frac{dC_1}{dx} &= -k_{1,2}\cdot C_1\\ \frac{dC_2}{dx} &= +k_{1,2}\cdot C_1 - \left(k_{2,3}+k_{2,4}\right)\cdot C_2\\ \frac{dC_3}{dx} &= +k_{3,5}\cdot C_3,\end{aligned} \tag{2}$$

where $C_{1,0} = C_{2,0} = C_{3,0}$ is the impurity concentration in raw material (Table 2) and $C_{4,0} = C_{5,0} = 0$.

Rewriting the equation system (2) in the matrix notation and assuming the algebraic feature $\sum_{i=1;i\neq j}^{N} k_{i,j} = k_{i,i}$, with the intent of achieving uniformity in the indexes of the array elements, we have

$$\begin{bmatrix} -k_{1,1} & 0 & 0\\ k_{1,2} & -k_{2,2} & 0\\ 0 & k_{2,3} & -k_{3,3}\end{bmatrix}\cdot\begin{bmatrix} C_1\\ C_2\\ C_3\end{bmatrix} = \begin{bmatrix}\dfrac{dC_1}{dx}\\ \dfrac{dC_2}{dx}\\ \dfrac{dC_3}{dx}\end{bmatrix}. \tag{3}$$

By applying the Laplace transform [13] in (3) and inverting the $[k]$ matrix,

$$\begin{bmatrix}\overline{C_1}(s)\\ \overline{C_2}(s)\\ \overline{C_3}(s)\end{bmatrix} = \frac{1}{\Delta}\cdot\begin{bmatrix}(s+k_{2,2})\cdot(s+k_{3,3}) & 0 & 0\\ k_{1,2}\cdot(s+k_{3,3}) & (s+k_{1,1})\cdot(s+k_{3,3}) & 0\\ k_{1,2}\cdot k_{2,3} & k_{2,3}\cdot(s+k_{1,1}) & (s+k_{1,1})\cdot(s+k_{2,2})\end{bmatrix}\cdot\begin{bmatrix}C_{1,0}\\ C_{2,0}\\ C_{3,0}\end{bmatrix}, \tag{4}$$

where $\overline{C_i}(s) = \mathscr{L}(C_i(x))$ is the Laplace transformation of $C_i(x)$ by changing the "x variable" to one in "s-space" and $\Delta = (s+k_{1,1})\cdot(s+k_{2,2})\cdot(s+k_{3,3})$. Hence,

$$\begin{bmatrix}\overline{C_1}(s)\\ \overline{C_2}(s)\\ \overline{C_3}(s)\end{bmatrix} = \begin{bmatrix}\dfrac{(s+k_{2,2})\cdot(s+k_{3,3})}{(s+k_{1,1})\cdot(s+k_{2,2})\cdot(s+k_{3,3})}\cdot C_{1,0}\\ \dfrac{k_{1,2}\cdot(s+k_{3,3})\cdot C_{1,0}+(s+k_{1,1})\cdot(s+k_{3,3})\cdot C_{2,0}}{(s+k_{11})\cdot(s+k_{2,2})\cdot(s+k_{3,3})}\\ \dfrac{k_{1,2}\cdot k_{2,3}\cdot C_{1,0}+k_{2,3}\cdot(s+k_{1,1})\cdot C_{2,0}+(s+k_{1,1})\cdot(s+k_{2,2})\cdot C_{3,0}}{(s+k_{11})\cdot(s+k_{2,2})\cdot(s+k_{3,3})}\end{bmatrix}. \tag{5}$$

Finally, applying the inverse of Laplace transformation, $C_i(x) = \mathscr{L}^{-1}(C_i(s) = P_i(s)/Q(s))$, using the Heaviside algorithm, where $Q(s) = \Delta$ and $P_i(s)$ is the numerator elements of the matrix product (6), then we have

$$C_1(x) = C_{1,0}\cdot e^{-k_{1,1}\cdot x} \tag{6}$$

$$\begin{aligned}&C_2(x)\\ &= \frac{k_{1,2}\cdot C_{1,0}}{k_{2,2}-k_{1,1}}\cdot e^{-k_{1,1}\cdot x} + \left(\frac{k_{1,2}\cdot C_{1,0}}{k_{1,1}-k_{2,2}} + C_{2,0}\right)\cdot e^{-k_{2,2}\cdot x}\end{aligned} \tag{7}$$

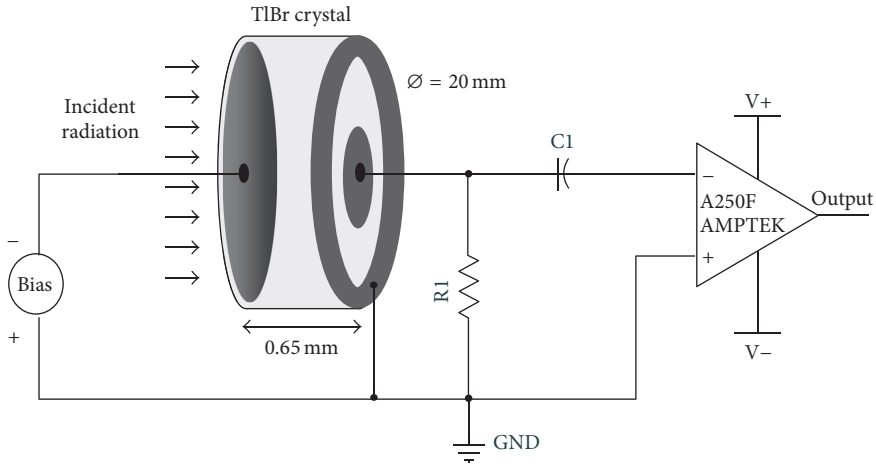

Figure 2: TlBr detector and preamplifier connections.

$$
\begin{aligned}
&C_3(x) \\
&= \frac{k_{1,2}\cdot k_{2,3}\cdot C_{1,0}}{(k_{2,2}-k_{1,1})\cdot(k_{3,3}-k_{1,1})}\cdot e^{-k_{1,1}\cdot x} \\
&\quad + \left(\frac{k_{1,2}\cdot k_{2,3}\cdot C_{2,0}}{(k_{1,1}-k_{2,2})\cdot(k_{3,3}-k_{2,2})} + \frac{k_{2,3}\cdot C_{2,0}}{k_{3,3}-k_{2,2}}\right) \\
&\quad \cdot e^{-k_{2,2}\cdot x} \\
&\quad + \left(\frac{k_{1,2}\cdot k_{2,3}\cdot C_{3,0}}{(k_{1,1}-k_{3,3})\cdot(k_{2,2}-k_{3,3})} + \frac{k_{2,3}\cdot C_{2,0}}{k_{2,2}-k_{3,3}} + C_{3,0}\right) \\
&\quad \cdot e^{-k_{3,3}\cdot x}.
\end{aligned}
\tag{8}
$$

The two end line compartments C_4 and C_5 have their cumulative impurities determined as follows:

$$C_4(x) = k_{2,4}\cdot\int_{x=0}^{x} C_2(x)\,dx \tag{9}$$

$$C_5(x) = k_{3,5}\cdot\int_{x=0}^{x} C_3(x)\,dx. \tag{10}$$

In summary, $C_i(x)$ is the experimental concentration of impurities in the crystal region i after the xth repetition of crystal growth, $C_{i,0}$ is the initial condition measured, experimentally, in raw material, and $k_{i,j}$ is the constant migration of impurities, determined by the nonlinear least-squares method. In this study, the compartmental calculations were made with Anacomp software [14–16].

The crystalline quality of the TlBr crystal was analyzed by X-ray diffraction (XRD). X-ray diffraction patterns were obtained in a Siemens (D5005) diffractometer with CuKα radiation (2θ ranging from 20° to 60°). The two sample slices from the middle crystal were prepared as a detector according to procedures described previously [7, 17, 18]. The crystal was sliced in wafers, cut transversally to direction (110), using a diamond saw, and lubricated with glycerine during the process. Crystals were cut slowly to have less damage and smaller depths in the resulting layers. Polishing, cleaning, and electrode painting were carried out, subsequently, without pause to avoid humidity deposition. The electrodes were made with colloidal carbon painting, Viatronix™. The final dimensions of the crystal wafers were, approximately, 20 mm diameter and 0.65 mm thickness. The detectors were made with a central electrode (anode), plus a ring electrode surrounding the anode electrode. The anode electrode diameter is about 3 mm and the ring electrode is around 4 mm internal diameter plus, approximately, 10 mm external diameter. The area for each electrode was defined from the painting mask electrode area and the thickness, with a micrometer. Figure 2 shows a schematic diagram of the detector and its connection to the preamplifier. The output from A250F charge sensitive preamplifier was connected to a 450 EG&G Ortec Research Amplifier at 10 μs shaping time and to EG&G 918A Multichannel Analyzer, to obtain the pulse height spectra. The detector signal is from an electron collector. TlBr crystal detectors were excited under a 59 keV ^{241}Am gamma source, biased with 400 V. For resistivity measurements, the ring electrodes were disconnected and the bias current was measured with a 619 Keithley Multimeter. All measurements were carried out at room temperature, 24 ± 2°C.

3. Results and Discussion

The X-ray diffraction pattern of TlBr salt exhibited a complete set of reflections (Figure 3(a)), while the typical X-ray diffraction pattern of TlBr crystals grown in this work presented only a reflection line (Figures 3(b) and 3(c)). The diffractogram indicates that the crystal is preferentially oriented in the (110) direction (Figures 3(b) and 3(c)). It is worthwhile to observe that there was no other crystalline phase in the grown crystal since all detected peaks corresponded to the TlBr peaks oriented in the (110) direction. These results are in agreement with the literature [4, 10].

In the classical approach, to determine the calculation of the segregation coefficient k, some idealized hypotheses are assumed [19]: (i) the concentration of the impurity in the raw material is constant in all the extension of its distribution in the crucible; (ii) the ingot cross section is

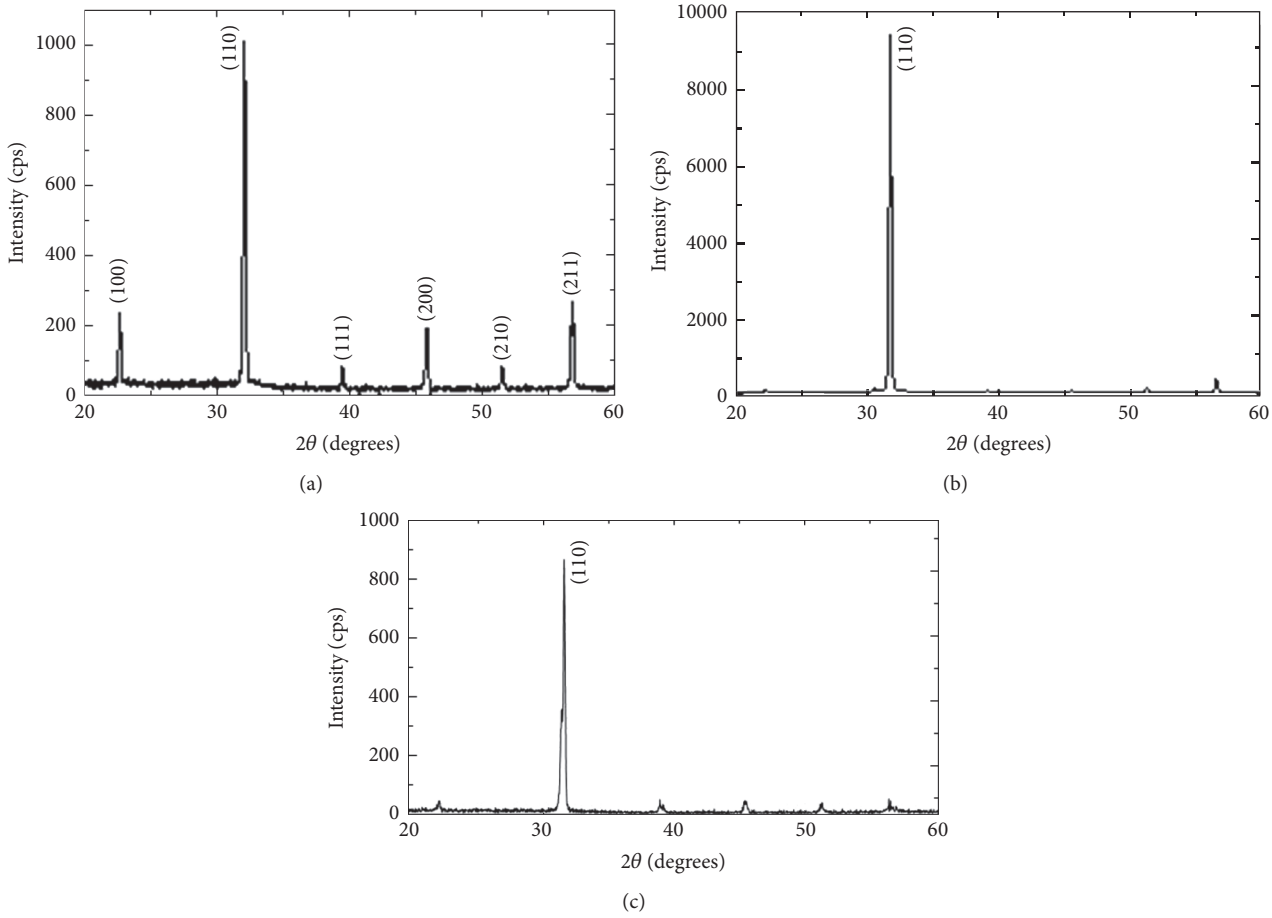

Figure 3: X-ray diffraction of TlBr powder (a) and TlBr crystal (b).

constant; (iii) the segregation coefficient is constant along the ingot length; (iv) the initial concentration in each i region of the ingot corresponds to the sum of the entire ingot, divided by the number of region sections; (v) the ingot length should be greater than the melting zone length, in order to drag impurities based on solubility differences of the solid-liquid phase. If all of these conditions are met, then the predictable mathematical model described in (11) may be used to calculate the concentration C_i, after zone refining:

$$C_i = C_0 \times \left[1 - (1 - k) \times e^{-k\cdot(i/l)}\right], \tag{11}$$

where C_i is the concentration of the impurity in the ith position along the ingot; C_0 is its initial concentration; k is the segregation coefficient; and l is the melting zone length. Due to the experimental particularities of the Bridgman purification used in this work, the following requirements mentioned previously are not established: (1st) in the crystal growth by the Bridgman technique, the raw material needs to be fully melted previously, which is in divergence with the hypothesis number (v); (2nd) in order to promote the nucleation, the growth crucible should be, preferably, cone-shaped, disregarding the hypothesis number (ii); (3th) due to the methodology applied, at each full melting, a fraction of the impurities, located in the top region, can recirculate by the Brownian movement, thereby reducing the efficiency of purification. To avoid this effect and to improve the quality of the purification process, the crucible of growth is opened and the upper portion of the crystal is cut and removed. Besides, to evaluate the effect of the impurities on the crystal performance as a radiation detector, samples were taken from the middle of the crystal, considered the prime region. Thus, due to these restrictions, the mathematical model based on zone refining, described by (11), is not suitable.

The basic assumptions applied to the formulation of the model described in Figure 1 and (6)–(10) were as follows: (i) the segregation coefficient $k < 1$ (i.e., the measured impurities are more soluble in the molten fraction of the crystal); (ii) initially, the impurity concentrations in the three regions (compartments), 1 to 3, are equal to the salt used as raw material and the initial concentrations in compartments 4 and 5 are both equal to zero; (iii) the migration coefficient $k_{i,j}$ is constant, independent of the crystal growth repetition number x (i.e., the quantity of impurities that migrate from region i to region j is proportional to their concentration in region i); and, finally, (iv) $k_{1,2} = k_{2,3}$. This algebraic feature allows a reduction in the number of variables to be determined by the nonlinear least-squares method [20];

Table 1: Three impurity concentrations (ppm) in the TlBr salt and in the top and middle regions of the TlBr crystal, by ICP-MS. The values represent the mean one standard deviation ($N = 10$ samples).

TlBr origin			Crystal region	Impurities elements (ppm)		
				Ba	Ca	Li
Salt 1	Bridgman growth step		Raw material	**5.46 ± 0.10**	**8.99 ± 0.12**	**2.39 ± 0.10**
		First	Top	5.36 ± 0.12	8.58 ± 0.13	2.34 ± 0.14
			Middle	4.93* ± 0.12	8.28* ± 0.07	2.05 ± 0.12
		Second	Top	6.38* ± 0.13	8.49 ± 0.10	3.00* ± 0.12
			Middle	6.09* ± 0.11	8.16* ± 0.13	3.04* ± 0.11
		Third	Top	5.49 ± 0.11	8.13* ± 0.09	2.76 ± 0.11
			Middle	3.05* ± 0.15	6.88* ± 0.12	1.88* ± 0.12
Salt 2	Bridgman growth step		Raw material	**9.64 ± 0.11**	**7.69 ± 0.09**	**1.92 ± 0.10**
		First	Top	9.25* ± 0.09	8.03* ± 0.09	1.61* ± 0.12
			Middle	9.10* ± 0.11	7.63* ± 0.10	1.60* ± 0.07
		Second	Top	9.11* ± 0.12	7.62 ± 0.12	1.54* ± 0.11
			Middle	8.96* ± 0.10	7.49 ± 0.012	1.40* ± 0.06
		Third	Top	9.02* ± 0.09	7.45* ± 0.11	1.57* ± 0.09
			Middle	8.68* ± 0.08	6.96* ± 0.12	1.33* ± 0.12

*There is a statistical difference between sample value and the initial concentration of raw salt ($p < 0.05$).

Table 2: Impurity migration coefficients.

Impurities	Transfer coefficient	TlBr Powder 1 (x^{-1})[a]	TlBr Powder 2 (x^{-1})[a]
Barium	$k1, 2 = k2, 3$	0.35 ± 0.01[b]	0.057 ± 0.003[b]
	$k2, 4$	0.074 ± 0.013[b]	0.037 ± 0.003[b]
	$k3, 5$	0.26 ± 0.01[b]	0.083 ± 0.003[b]
Calcium	$k1, 2 = k2, 3$	0.29 ± 0.09[b]	0.17 ± 0.02[b]
	$k2, 4$	0.0076 ± 0.0463[b]	0.00070 ± 0.00887[b]
	$k3, 5$	0.311 ± 0.086[b]	0.18 ± 0.02[b]
Lithium	$k1, 2 = k2, 3$	0.21 ± 0.51[b]	0.056 ± 0.356[b]
	$k2, 4$	0.004 ± 0.200[b]	0.14 ± 0.02[b]
	$k3, 5$	0.12 ± 0.45[b]	0.15 ± 0.34[b]
Mean ± SD	$k1, 2 = k2, 3$	**0.283 ± 0.029**	**0.094 ± 0.066**

[a]x: number of repeated Bridgman growths.
[b]Regression asymptotic error (the calculated error in the last iteration).

moreover, this hypothesis is in agreement with the same rule (hypothesis number (iii)), used in the formulation of the zone refined model (k without index in (11)). The constants $k_{2,4}$ and $k_{3,5}$ depend on the size of the sliced material removed from the crystal and were numerically estimated by the fitting regression process.

The concentration of three ions (Ca, Ba, and Li) found in the crystal grown three times, sequentially, for the two salts, is presented in Table 1 and Figure 4. Comparisons among initial impurities from the two salts (raw materials) suggest that Salt 1 has less Ba (5.46 ± 0.10 ppm) than Salt 2 (9.64 ± 0.11 ppm), while both salts have similar concentration of Ca (8.99 ± 0.12 ppm for Salt 1 versus 7.69 ± 0.09 ppm for Salt 2) and Li (2.39 ± 0.10 ppm for Salt 1 versus 1.92 ± 0.10 ppm for Salt 2).

For Salt 1, after the first purification, the amount of impurities in the top region was not, significantly, different from the raw salt. However, for Salt 2, major differences were found for all three impurity elements in the crystal top region. In the case of the crystal middle region, a significant difference in the crystal impurity concentrations was observed for almost all impurities, compared to those found in the raw material (Salts 1 and 2).

According to Table 1, for Salt 1, the reduction level of the impurities in the crystal middle region, after the third growth, was of 44% (1 − (3.05/5.46)) for Ba, 23% (1 − (6.88/8.99)) for Ca, and 21% (1 − (1.88/2.39)) for Li. On the other hand, for the second salt, the results were worse, with 10% (1 − (8.68/9.64)) for Ba, 9% (1 − (6.96/7.69)) for Ca, and 31% (1 − (1.33/1.92)) for Li. Comparing the averages of $k_{1,2} = k_{2,3}$ (Table 2) for the two salts, similar results can be reached. It should be emphasized that, in the compartmental theory, there is not a rigorous commitment that k parameter should be equal among the regions. However, for the same raw salt,

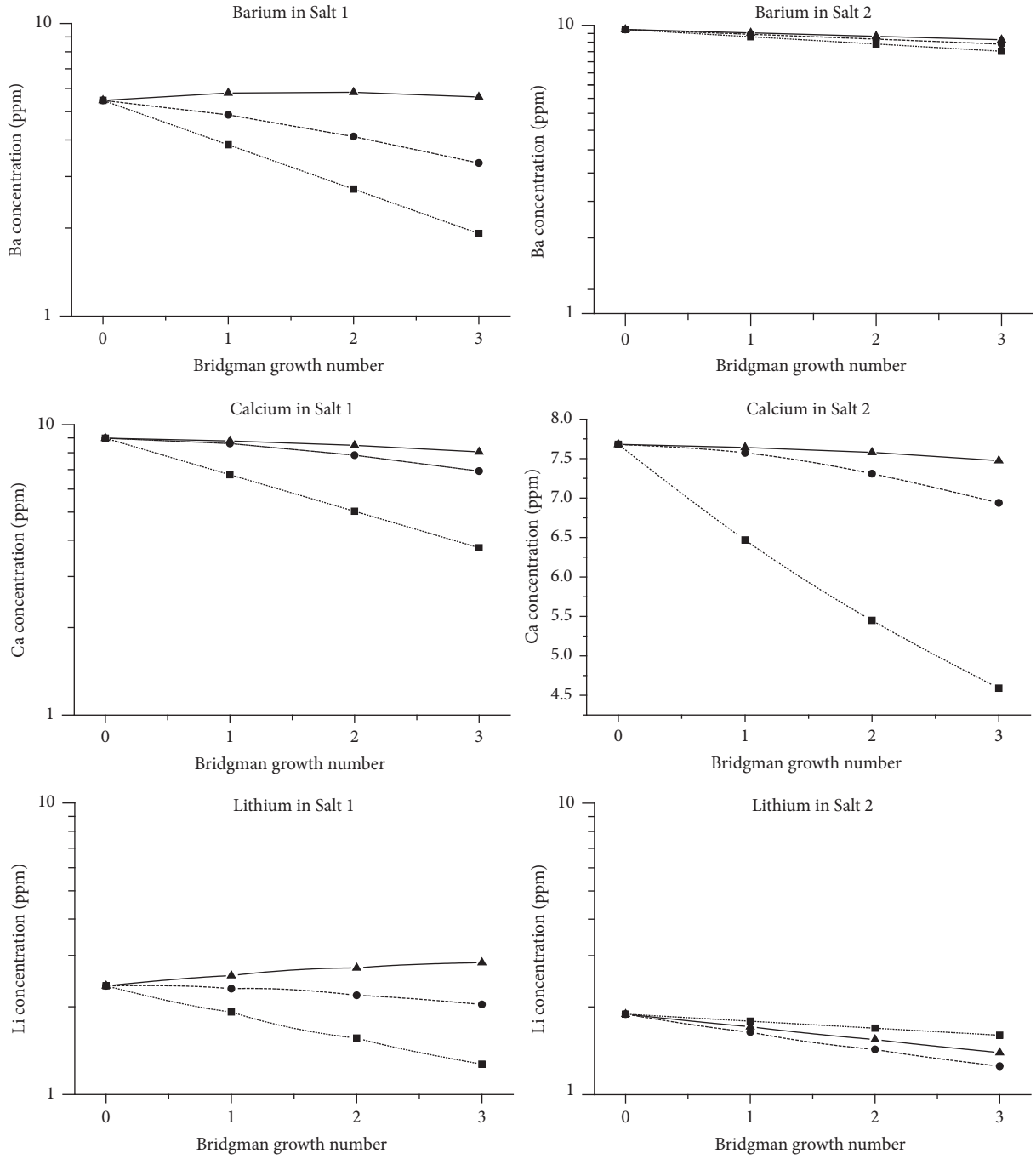

Figure 4: Concentration of impurity ions in different regions of crystals. ■ bottom region: compartment C_1; ● middle region: compartment C_2; ▲ top region: compartment C_3. Values were calculated theoretically from model described in Figure 1 and (7), (8), and (9).

the $k_{1,2} = k_{2,3}$ values found were close to each other, and thus this assumption may be made. The difference in the mean values of these two groups (0.28 ± 0.07 versus 0.094 ± 0.07) is greater than what could be expected by chance; hence, there is a statistically significant difference between Salts 1 and 2 ($p = 0.0271$). These results suggest that some unknown factors, present in Salt 2, slow down the separation of impurities along the crystal and, consequently, the choice of the commercial raw salt should be made experimentally, independent of its nominal declaration of purity.

The model shown in Figure 1 is valuable for quality control purposes. In such case, the $k_{i,j}$ parameters, which are associated with the impurity migration efficiency, may be an important auxiliary tool to design, optimize, and explain the results and processes involved in the purification of raw salt used to grow crystals. For example, to understand the rise in the concentration of impurities in the crystal middle region, increased in the second Bridgman growth (Figures 4 and 5), despite a seeming contradiction, this occurrence can be predicted and quantified by the compartmental analysis.

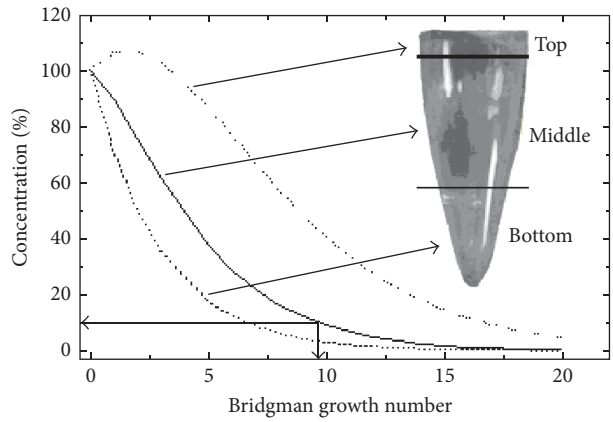

Figure 5: Predictive concentration (%) for Salt 1 as a function of repetition number of Bridgman growth, curves calculated from the model of Figure 1 and (7), (8), and (9). To achieve 10% of initial concentration in the crystal middle region, approximately 10 steps are required.

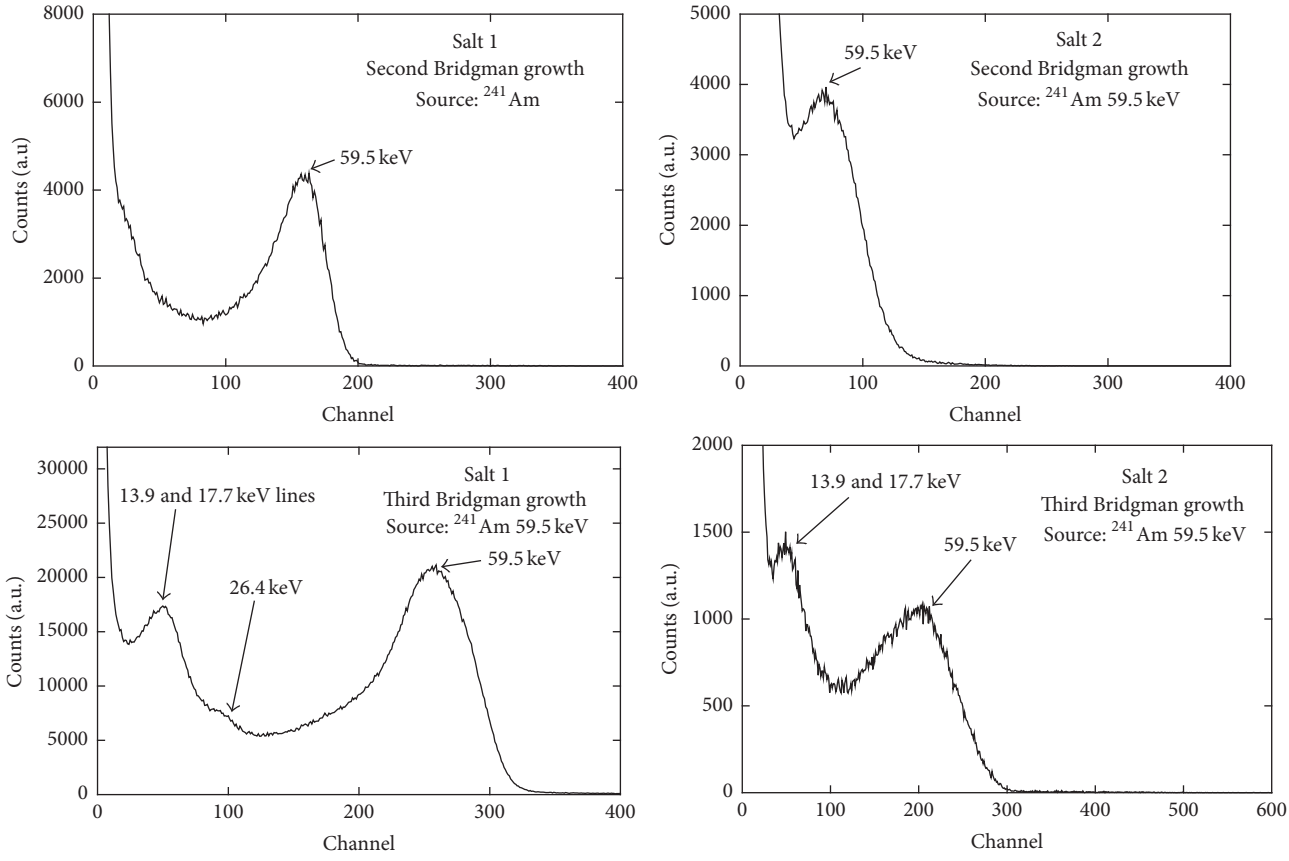

Figure 6: TlBr detector energy spectra under ^{241}Am excitations. Detectors were prepared using TlBr samples from the middle region of the crystals grown twice and three times.

As shown in Figure 4, the impurities concentration $C_2(x = 2) \sim 110\%$, in the middle of the crystal, is greater than that found in the raw material ($C_{2,0} = 100\%$). The proposed model (Figure 1) provides the comprehension of this effect, since it is capable of forecasting the notion that the impurities located in the prior region migrate to the subsequent region, contributing to the increase of their concentration. Thus, the $k_{i,j}$ parameter is valuable to represent the effectiveness of the purification technique. Moreover, the model may be useful to predict the repetition number of Bridgman growths required to reduce the impurities to a level, for example, of 10% of the raw salt ($C_0 = 100\%$). In the present work, approximately 10 repetitions of the Bridgman growth would be necessary (Figure 5) to achieve this requirement.

For the purpose of analyzing the effectiveness of the purification process, a spectrometric analysis was performed

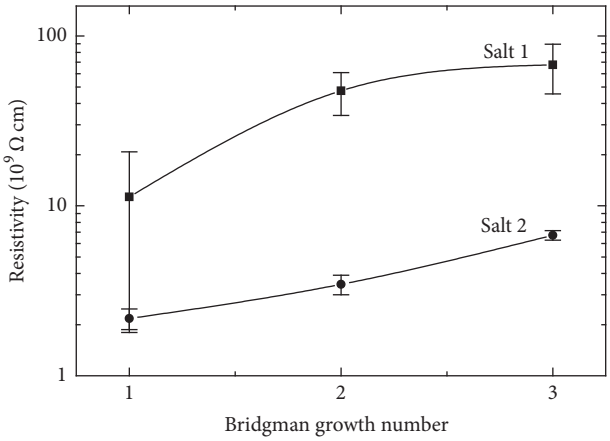

Figure 7: Resistivity of the TlBr detector from crystal middle region (slice ~ 0.65 mm thick) as a function of the repetition number of Bridgman growth. The bar error represents one standard deviation ($N = 3$ samples).

Table 3: Resistivity values for TlBr detectors prepared from the crystal grown once, twice, and three times by the repeated Bridgman method. The samples used are from crystal middle region.

Bridgman growth	Resistivity (10^9 Ωcm)	
	Salt 1	Salt 2
First	11.3 ± 9.5	2.17 ± 0.30
Second	47.5 ± 13.4	3.45 ± 0.45
Third	67.5 ± 21.9	6.72 ± 0.43

and the results were compared with the efficiency of the purification (Figure 6). The pulse height spectra obtained suggest a significant improvement in their profiles when the purification number is increased. For the TlBr crystal grown once, it was not possible to observe the photopeak profile because the pulses generated fall in the electrical noise region. For the TlBr grown twice, only the photopeak of 59 keV of ^{241}Am gamma source can be observed. For the third grown crystal, some ranges of energy below 59 keV can be observed. Both starting materials (Salts 1 and 2) show similar spectrum details, although the raw material of Salt 1 shows, systematically, better results, mainly in terms of resistivity values (Table 3 and Figure 7). The resistivity found in this work is similar to that described by Hitomi et al. [6].

The resistivity curve showed a positive slope (Figure 7), tending to achieve a plateau. Although both salts had, nominally, the same initial purity (99.99%), the crystals grown showed resistivity differences of, approximately, 10 times. The resistivity of the crystals from Salt 1 presented values 10 times higher than crystals from Salt 2 (Figure 7 and Table 1). There is evidence that Salt 1 has better performance in all parameters studied: this fact could be associated with the resistivity of crystals. In fact, the lowest resistivity of the crystals produced with Salt 2 could be correlated with its lower performance. However, comparing the spectrometric performance, while the crystals from Salt 1 first growth (high resistivity) did not show any detailed spectrum, in contrast, Salt 2 second and third growths (low resistivities) presented good detailed spectra (Figure 6). This fact suggests that the resistivity did not seem to have a fundamental role in characterizing the spectrum quality of the crystal. Vieira et al. [7]. described a similar observation in their result of resistivity measurements correlated to the number of zone-refining passes carried out in the TlBr purification. Further studies should be carried out to elucidate these results.

4. Conclusion

The repeated Bridgman method was efficient to purify the TlBr crystals and to improve their performance as radiation detectors. A compartmental model defined by linear differential equations may be used to calculate the coefficients for the migration of impurities. This is useful for predicting the number of repetitions by Bridgman growth needed to achieve a desirable concentration value. The resistivity showed a positive slope, tending to reach a plateau after the third growth. The TlBr resistivity above ~3 MΩ was almost unaffected by the number of repetitions when growing crystals by Bridgman technique.

Competing Interests

The authors declare that they have no competing interests.

Acknowledgments

The authors are grateful to CNPq for the financial support and grants.

References

[1] D. S. Macgregor and H. Hermon, "Room-temperature compound semiconductor radiation detectors," *Nuclear Instruments and Methods in Physics Research Section A*, vol. 395, no. 1, pp. 101–124, 1997.

[2] I. B. Oliveira, F. E. Costa, J. F. D. Chubaci, and M. M. Hamada, "Purification and preparation of TlBr crystals for room temperature radiation detector applications," *IEEE Transactions on Nuclear Science*, vol. 51, no. 3, pp. 1224–1228, 2004.

[3] K. Hitomi, M. Matsumoto, O. Muroi, T. Shoji, and Y. Hiratate, "Characterization of thallium bromide crystals for radiation detector applications," *Journal of Crystal Growth*, vol. 225, no. 2-4, pp. 129–133, 2001.

[4] V. Kozlov, H. Andersson, V. Gostilo et al., "Improvements and problems of Bridgman-Stockbarger method for fabrication of TlBr single crystal detectors," *Nuclear Instruments and Methods in Physics Research A*, vol. 607, no. 1, pp. 126–128, 2009.

[5] M. S. Kouznetsov, I. S. Lisitsky, S. I. Zatoloka, and V. V. Gostilo, "Development of the technology for growing TlBr detector crystals," *Nuclear Instruments and Methods in Physics Research Section A: Accelerators, Spectrometers, Detectors and Associated Equipment*, vol. 531, no. 1-2, pp. 174–180, 2004.

[6] K. Hitomi, T. Onodera, and T. Shoji, "Influence of zone purification process on TlBr crystals for radiation detector fabrication," *Nuclear Instruments and Methods in Physics Research Section A: Accelerators, Spectrometers, Detectors and Associated Equipment*, vol. 579, no. 1, pp. 153–156, 2007.

[7] C. L. Vieira, F. E. Costa, and M. M. Hamada, "Effect of etching on the TlBr crystal surface and its radiation response," in *Proceedings of the International Nuclear Atlantic Conference, VIII ENAN Proceedings*, Santos, Brazil, October 2007.

[8] J. Vaitkus, V. Gostilo, R. Jasinskaite et al., "Investigation of degradation of electrical and photoelectrical properties in TlBr crystals," *Nuclear Instruments and Methods in Physics Research, Section A: Accelerators, Spectrometers, Detectors and Associated Equipment*, vol. 531, no. 1-2, pp. 192–196, 2004.

[9] F. E. Da Costa, P. R. Rela, I. B. De Oliveira, M. C. C. Pereira, and M. M. Hamada, "Surgical gamma probe with TlBr semiconductor for identification of sentinel lymph node," *IEEE Transactions on Nuclear Science*, vol. 53, no. 3, pp. 1403–1407, 2006.

[10] V. Kozlov, M. Heikkilä, P. Kostamo, H. Lipsanen, and M. Leskelä, "TlBr purification and single crystal growth for the detector applications," *Nuclear Instruments and Methods in Physics Research, Section A: Accelerators, Spectrometers, Detectors and Associated Equipment*, vol. 633, no. 1, pp. S72–S74, 2011.

[11] T. Tada, K. Hitomi, T. Tanaka et al., "Digital pulse processing and electronic noise analysis for improving energy resolutions in planar TlBr detectors," *Nuclear Instruments and Methods in Physics Research A*, vol. 638, no. 1, pp. 92–95, 2011.

[12] A. Ray, H. M. Smith III, and N. M. Haegel, "Temperature dependence of the indirect bandgap in thallium bromide from cathodoluminescence spectroscopy," *Journal of Applied Physics*, vol. 115, no. 16, Article ID 163709, 2014.

[13] M. Abramowitz and I. A. Stegun, "Laplace transform," in *Handbook of Mathematical Functions with Formulas. Graphs and Mathematical Tables*, chapter 29, pp. 1019–1030, Dover, New York, NY, USA, 9th edition, 1972.

[14] M. Berman, "The formulation and testing of models," *Annals of the New York Academy of Sciences*, vol. 108, no. 1, pp. 182–194, 1963.

[15] A. Rescigno and G. Segre, *Drug and Tracer Kinetics*, Blaisdell Publishing, Waltham, Mass, USA, 1966.

[16] C. H. Mesquita, *AnaComp—Compartmental Analysis Aided by Computer—User Manual*, Instituto de Pesquisas Energéticas e Nucleares, São Paulo, Brazil, 1994.

[17] F. E. da Costa, C. H. de Mesquita, and M. M. Hamada, "Temperature dependence in the long-term stability of the TlBr detector," *IEEE Transactions on Nuclear Science*, vol. 56, no. 4, pp. 1817–1822, 2009.

[18] R. A. Santos, J. B. R. Silva, R. F. Gennari et al., "Multi-elemental segregation analysis of thallium bromide impurities purified by the repeated bridgman technique," *IEEE Transactions on Nuclear Science*, pp. 4118–4123, 2012.

[19] W. G. Pfann, *Zone Melting*, John Wiley & Sons, New York, NY, USA, 1958.

[20] P. R. Bevington, *Data Reduction and Error Analisys for the Physical Sciences*, McGraw-Hill, New York, NY, USA, 1969.